



Full paper/Mémoire

Preparation, characterization, and hydrogenation activity of new Rh⁰–MCM-41 catalysts prepared from as-synthesized MCM-41 and RhCl₃

Maya Boutros ^{a, b, *}, Georges Moarbess ^b, Thomas Onfroy ^{c, d}, Franck Launay ^c

^a Université libanaise, Laboratoire de chimie physique des matériaux (LCPM), Faculté des sciences II, Campus Fanar, BP 90696, Jdeideh, Lebanon

^b Université libanaise, Faculté des sciences II, Département de chimie et biochimie, Campus Fanar, BP 90696, Jdeideh, Lebanon

^c Sorbonne Université, CNRS, Laboratoire de réactivité de surface, LRS, Campus Pierre-et-Marie-Curie, 75005 Paris, France

^d Normandie Université, ENSICAEN, UNICAEN, CNRS, Laboratoire "Catalyse et Spectrochimie", 14050 Caen, France

ARTICLE INFO

Article history:

Received 6 November 2017

Accepted 11 January 2018

Available online 19 February 2018

Keywords:

MCM-41

Rhodium

Template-ion exchange

Ethanol

Hydrogenation

ABSTRACT

Impregnation of as-synthesized MCM-41 silica by ethanolic solutions of rhodium(III) chloride was tested as an alternative to its introduction into the synthesis gel to get, after calcination and reduction by H₂, highly dispersed metal(0) nanoparticles throughout the mesopores network. Rh(III) and Rh(0)-based solids thus obtained were analyzed by infrared spectroscopy, elemental analysis, transmission electron microscopy, N₂ sorption, and X-ray diffraction. Materials with 1.6 wt % of rhodium could be obtained as a result of CTA⁺/Rh³⁺ exchange. The determining role of CTA⁺ was emphasized through blank experiments. In a second series of materials, ethanol was also exploited for its ability to reduce Rh(III). All Rh(0)-based solids were tested as catalysts in the hydrogenation of styrene under mild temperature and pressure conditions. Catalysis performances of the most efficient sample (reduced by H₂) were further compared with those of a very similar material prepared by the introduction of Rh(III) directly into the synthesis gel of MCM-41 silica. Better *cis* selectivities in the hydrogenation of disubstituted arene derivatives were achieved with materials issued from the new preparation method.

© 2018 Académie des sciences. Published by Elsevier Masson SAS. All rights reserved.

1. Introduction

Supported rhodium(0) nanoparticles efficiently catalyze the hydrogenation of aromatic rings under rather soft temperature and pressure conditions [1]. Main applications include, for example, obtaining cyclohexane from benzene, the decrease in the fraction of aromatic compounds in gasolines, or the one-step preparation of substituted cyclohexane derivatives with stereoselectivity challenges. However, rhodium is particularly expensive. Efforts must be made to minimize the metal loading on the catalyst

supports. Porous carbonaceous and oxide materials with large specific surfaces are privileged as well as protocols incorporating a large number of active atoms. Usually, strategies implemented to increase the dispersion of rhodium nanoparticles rely on the use of controlled reduction processes after the deposition of the metal precursor or before (colloidal approach [2–5]). In the first approach, better dispersions are more easily obtained for carriers bearing either intrinsic [6] or added [7–13] anchoring sites.

As far as mesostructured supports are concerned, the introduction of the metal source in the synthesis gel has also been implemented using either inorganic salts [6,14,15] or metal soaps [16]. Often, structural and textural

* Corresponding author.

E-mail address: boutrosmaya@hotmail.com (M. Boutros).

parameters of the resulting solids are seriously degraded. For materials of the MCM-41 type, another strategy affording supports with structural and textural parameters of high quality as well as the incorporation of significant amounts of active phases uses silicate species (I^-) on the internal surface of the preformed as-synthesized solid as anchoring sites. Indeed, the metal cationic precursor is expected to exchange with the template (cetyltrimethylammonium ion (CTA^+) denoted as S^+) leading to the metal uptake and also to a cleaner removal of organics as compared to calcination protocols. Such a pathway was used for the first time to prepare Mn–MCM-41 [17]. Since this so-called template-ion exchange (TIE) method has been extended to prepare MCM-41 type materials incorporating Cr, Fe, Co, V, Ti, Ni, and so forth [18–38]. Usually the resulting solids are calcined and the heteroelements introduced are tested in oxidation or acid catalysis tests. Fewer studies deal with the use of this strategy to get zerovalent metal particles and locate them within the mesopores [34,35].

In the present article, rhodium(0) nanoparticles useful for the hydrogenation of aromatic substrates under mild conditions were prepared by this “TIE” approach with or without any additional reducing agent. Parameters influencing the amount and location of Rh(0) in the final materials were studied. The structural and textural properties of the resulting rhodium-containing mesoporous silicas, the size and the dispersion of the metal nanoparticles, and their catalytic performances were compared to those of Rh^0 –MCM-41 prepared through the incorporation of Rh(III) ions in the synthesis gel of MCM-41 [6].

2. Experimental section

2.1. Synthesis of Rh^0 –MCM-41 materials

2.1.1. From the as-synthesized MCM-41 and ethanolic rhodium solutions

Pure silica MCM-41 (MCM-41) was synthesized according to the method reported by Brühwiler and Frei [39] using cetyltrimethylammonium bromide (CTAB) as a templating agent and tetraethoxysilane (TEOS) as a silicon source. Amounts of silicon, carbon, and nitrogen in the as-synthesized MCM-41 (as-MCM-41), that is, 29.6, 21.6, and 1.3 wt %, respectively (elemental analysis) are consistent with the presence of CTAB (C/N = 19.4 instead of 19) as the main organic component. In the present article, the amount of template (CTA^+) in the as-MCM-41 is considered to be ca. 26 wt %. Full extraction of CTA^+ was also performed for blank experiments using repeated extractions of the as-MCM-41 in the presence of NH_4NO_3 aqueous solutions [12,40]. The corresponding surfactant-free support was denoted as ext-MCM-41.

Targeted materials Rh^0 –MCM-41/ $t(y)$, named Rh^0 –M/ $t(y)$, were prepared in ethanol using $RhCl_3 \cdot xH_2O$ ($Rh = 40.79$ wt % corresponding to $x = 2.25$; Strem chemicals) as the rhodium source. The influence of the contact time (t) between as-MCM-41 and $RhCl_3 \cdot xH_2O$ and of the nominal Si/Rh molar ratio (y) was first tested. Hence, as-MCM-41 (1.0 g) was added to 40 mL of an ethanolic solution of rhodium(III) chloride. The resulting mixture was

stirred vigorously at 60 °C for $t = 3, 6,$ or 24 h and y value was varied from 135 to 35. Resulting Rh^{III} –M/ $t(y)$ solids were recovered through a filtration step, then washed with distilled water, dried at 40 °C for 24 h, and calcined in air, first at 300 °C for 2 h and then at 550 °C for 12 h (heating rate, 2 °C min^{-1}). For the sake of comparison, two blank materials, M/6(∞) ($y = \infty, t = 6$ h) and M/24(∞) ($y = \infty, t = 24$ h), were also prepared in the absence of rhodium.

The corresponding reduced materials of the first series, Rh^0 –M/ $t(y)$, were obtained through a dihydrogen treatment. In a typical experiment [6], the Rh^{III} –M/ $t(y)$ solid was preheated under oxygen flow (1.4 mL s^{-1}) from 25 to 300 °C (ramping rate, 60 °C h^{-1}), then 2 h under vacuum at 300 °C to obtain RhO_x species. After cooling, H_2 gas (0.83 mL s^{-1}) was passed through the sample while heating from 25 to 220 °C (ramping rate, 12 °C h^{-1}). The temperature was maintained at 220 °C for 1 h and hydrogen gas was then evacuated. Finally, the sample was further heated from 220 to 400 °C (ramping rate, 60 °C h^{-1}) and kept at 400 °C for 12 h before cooling to room temperature under vacuum.

Three other samples were obtained through the reduction of rhodium using boiling ethanol. Among them, Rh^0 –M/6(Et,78,2)/- and Rh^0 –M/6(Et,78,2)/c materials were prepared by a 2-h treatment of the intermediate solid, here Rh^{III} –M/6(70), either by increasing the temperature from 60 to 78 °C (case of Rh^0 –M/6(Et,78,2)/-) or by treating all the isolated calcined form of Rh^{III} –M/6(70) (corresponding to 1 g of as-MCM-41) by 40 mL of ethanol at 78 °C (case of Rh^0 –M/6(Et,78,2)/c). The third material, Rh^0 –M/6(Et,78,6), was prepared as Rh^0 –M/6(70) but using ethanol at 78 °C instead of 60 °C for 6 h. Conditions for the preparation of all the solids described in this study are summarized in Table 1.

2.1.2. By a direct hydrothermal synthesis method

The reference material obtained by direct hydrothermal synthesis, Rh^0 –M(1)/120, was prepared as described previously [6]. Hence, CTAB (2.2 g) was dissolved under slight warming (35 °C) in a mixture of 52 mL of distilled H_2O and 24 mL of 30 wt % aqueous ammonia. Rhodium chloride

Table 1

Rh-M/ $t(y)$ samples prepared from as-synthesized MCM-41 and ethanolic solution.

Samples	Sample preparation method	Reduction treatment	Nominal Si/Rh molar ratio	Contact time t (h)
Rh^0 –M/6(70)	TIE	H_2	70	6
Rh^0 –M/24(70)	TIE	H_2	70	24
Rh^0 –M/6(130)	TIE	H_2	130	6
Rh^0 –M/6(35)	TIE	H_2	35	6
Rh^0 –M(1)/120	DHT [6]	H_2	70	–
Rh^0 –M(Et,78,2)/-	TIE	EtOH	70	6 (60 °C) No isolation +2 (78 °C)
Rh^0 –M/6(Et,78,2)/c	TIE	EtOH	70	6 (60 °C) Isolation, calcination +2 (78 °C)
Rh^0 –M'/6(Et,78,6)	TIE	EtOH	70	6 (78 °C)

DHT, direct hydrothermal synthesis; TIE, template-ion exchange.

hydrate was introduced into the solution (6×10^{-4} mol), which was stirred for 15 min until it became clear. Then, 10 mL of TEOS was slowly added. The resulting gel was aged for 3 h at room temperature, then transferred into a Fluorinated Ethylene Polymer (FEP) bottle and was hydrothermally treated at 110 °C for 48 h. The solid product was filtered, washed with distilled water, dried at 60 °C for 24 h, calcined in air, first at 300 °C for 2 h and then at 550 °C for 12 h (heating rate was 2 °C min⁻¹), and reduced by H₂ using the procedure described in Section 2.1.1.

2.2. Characterization

The silicon, carbon, nitrogen, and rhodium compositions of the various materials were determined by Inductively Coupled Plasma - Atomic Emission Spectroscopy (ICPAES) in the "Centre national de la recherche scientifique" (CNRS) at Vernaison (France). Fourier transform infrared (FTIR) spectra were collected using a Bruker Vector 22 spectrophotometer (resolution of 2 cm⁻¹) with KBr pellets (4 wt % in KBr). CTA⁺ were quantified in the different uncalcined samples (Rh^{III}-M/*t*(*y*), M/6(∞), and M/24(∞) solids) by monitoring the area of ν(C-H) bands at 2854 and 2925 cm⁻¹ normalized against that of the ν(Si-O-Si) of the support at 800 cm⁻¹. Measurements performed on the materials before (as-MCM-41) and after the incorporation of rhodium were used to estimate the loss of surfactant (Δ*S*). The quantity (in moles) of surfactant removed per mole of rhodium incorporated (Δ*S*/Rh) was calculated by coupling IR data (Δ*S*) and elemental analyses of as-MCM-41 and Rh⁰-M/*t*(*y*) samples. X-ray diffraction (XRD) patterns were recorded between 1° and 7° (2θ) using a Bruker Advance D8 diffractometer with the Cu Kα radiation (λ = 0.15418 nm) with steps of 0.02° and a count time of 6 s at each point.

The specific surface area, pore volume, and pore diameter of calcined samples were determined from N₂ sorption data obtained at -196 °C using an ASAP 2010 Micromeritics instrument. Before the analysis, the samples were outgassed at 200 °C until a stable static vacuum of 2.10⁻³ Torr was reached. The pore diameter and specific pore volume were calculated according to the Barrett-Joyner-Halenda (BJH) model. The specific surface area was obtained by using the Brunauer-Emmett-Teller (BET) equation. Transmission electron analyses were performed using a JEOL 100CXII transmission electron microscope operated at an acceleration voltage of 100 kV. In some cases, the materials were included in a resin

(AGAR 100) and heated for 48 h at 60 °C, then thin (70 nm) sections cut with a Leica microtome (Ultracut UCT) were collected on carbon-coated copper grids.

2.3. Catalysis tests

Rh-containing samples were tested as catalysts in the hydrogenation of aromatic substrates at room temperature under atmospheric pressure (styrene) or at 1 MPa (disubstituted arene derivatives) of dihydrogen. Solids were first dispersed in hexane (10 mL) under magnetic stirring for 15 min before the introduction of the substrate (100 equiv metal⁻¹). Products were quantified with *n*-decane as an internal standard using a Delsi Nermag DN 200 gas chromatograph equipped with an SPB-5 capillary column and a flame ionization detector.

3. Results and discussion

As-MCM-41 used as the starting material was estimated to contain 9×10^{-4} mol g⁻¹ of CTA⁺ (see Section 2) with thus a maximum exchange capacity toward Rh³⁺ of 3×10^{-4} mol g⁻¹. Under these conditions, a minimum Si/Rh molar ratio expected was estimated to be 35.

3.1. Variations in the contact time (*t*) between as-MCM-41 and RhCl₃·xH₂O and in Si/Rh molar ratio (*y*)

First, three materials with nominal Si/Rh values (*y*) equal to 35, 70, and 130 were prepared by contacting as-MCM-41 and RhCl₃ 6 h in ethanol at 60 °C (see Rh^{III}-M/6(*y*) solids in Table 2). Resulting solids were characterized in their Rh(III) form (FTIR) and at the zerovalent state, that is, after calcination and H₂ treatment (XRD, N₂ sorption, and transmission electron microscopy [TEM]). For the discussion, they have also been compared with Rh⁰-M/24(70) resulting from a longer contact time (24 h) and two blank samples, M/6(∞) and M/24(∞), obtained in the absence of rhodium.

The evolution of the areas of the ν(C-H) bands of CTA in as-MCM-41 and uncalcined Rh^{III}-M/*t*(*y*), MCM-41/6, and MCM-41/24 materials is presented in Fig. 1. From comparisons with as-synthesized silica MCM-41, it is clear that no significant release of CTA⁺ was observed in the absence of rhodium (case of M/6(∞) and M/24(∞), Fig. 1(b) and (c)). In fact, loss of CTA⁺ over a period of 24 h (MCM-41/24) was less than 7 wt %. In the presence of rhodium, with Rh^{III}-M/

Table 2
Physicochemical properties of Rh⁰-M/*t*(*y*) samples synthesized in ethanol.

Samples	Si/Rh ^a	Rh (wt %)	Yield ^b (%)	Δ <i>S</i> /Rh ^c	S _{BET} (m ² g ⁻¹)	V _{pores} (cm ³ g ⁻¹)	D _p (nm)
Si-MCM-41	—	—	—	—	800	0.70	2.6
Rh ⁰ -M/6(70)	113	1.35	60	7	775	0.69	2.7
Rh ⁰ -M/24(70)	136	1.11	50	6	740	0.66	2.6
Rh ⁰ -M/6(130)	444	0.34	30	17	745	0.66	2.6
Rh ⁰ -M/6(35)	123	1.30	28	8	780	0.71	2.7
Rh ⁰ -M/6(70/70) ^d	100	1.55	35	7.5	770	0.68	2.7
Rh ⁰ -M(1)/120	120	1.30	58	—	720	0.63	2.7

^a Si/Rh experimental molar ratio.

^b Rh incorporation yield = [(Si/Rh nominal)/(Si/Rh exp)] × 100.

^c Mole of surfactant removed per mole of metal introduced.

^d As-MCM-41 was contacted twice for 6 h with an ethanolic solution of RhCl₃ (*y* = 70).

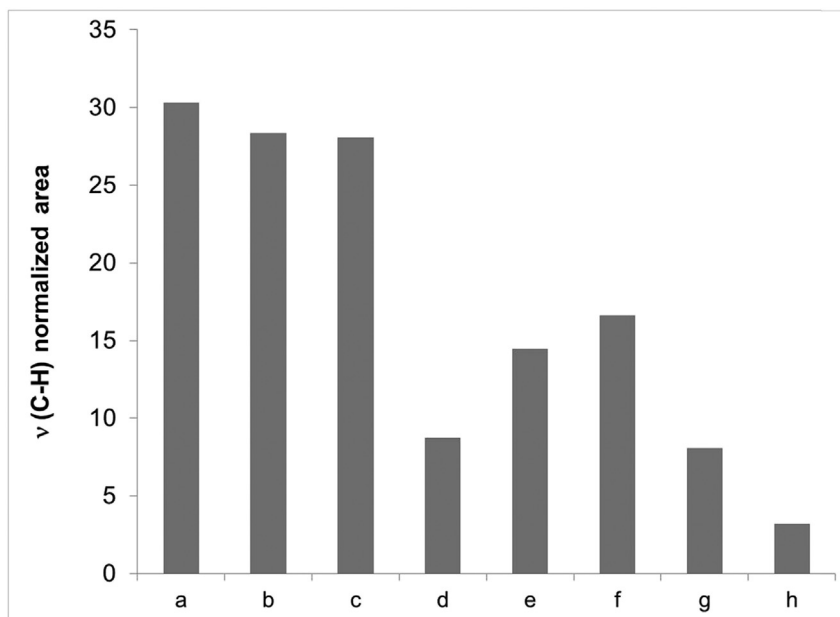


Fig. 1. Normalized $\nu(\text{C-H})$ area for the as-synthesized (a) MCM-41, (b) M/6(∞), (c) M/24(∞), (d) $\text{Rh}^{\text{III}}\text{-M}/6(130)$, (e) $\text{Rh}^{\text{III}}\text{-M}/6(70)$, (f) $\text{Rh}^{\text{III}}\text{-M}/24(70)$, (g) $\text{Rh}^{\text{III}}\text{-M}/6(35)$, and (h) $\text{Rh}^{\text{III}}\text{-M}/6(70/70)$.

6(130) and $\text{Rh}^{\text{III}}\text{-M}/6(70)$ samples (Fig. 1(d) and (e)), the normalized area of the $\nu(\text{C-H})$ bands decreased with an increase in the nominal amount of metal. However, additional quantities of rhodium ($\text{Rh}^{\text{III}}\text{-M}/6(35)$) did not lead to further surfactant removal (Fig. 1(g)). No significant difference between rhodium loadings (about 1.3 wt %) was also found for $\text{Rh}^0\text{-M}/6(70)$ and $\text{Rh}^0\text{-M}/6(35)$ samples, thus assessing a relationship between CTA^+ release and Rh^{3+} insertion. Regardless of the amount of rhodium, values of Rh loadings were lower than nominal ones. Incorporation yields of the metal vary between 30% and 60% (Table 2) with the maximum reached for Si/Rh = 70. Surfactant losses versus rhodium incorporation (expressed as $\Delta\text{S}/\text{Rh}$ values) in $\text{Rh}^{\text{III}}\text{-M}/6(y)$ samples were always superior to 3, the value expected for a true ion exchange between one Rh^{3+} and three CTA^+ . Indeed $\Delta\text{S}/\text{Rh}$ values varied from 17 for the smallest nominal metal loading ($\text{Rh}^{\text{III}}\text{-M}/6(130)$) to 7.5 for highest ones ($\text{Rh}^{\text{III}}\text{-M}/6(35)$). For $y = 70$, a longer contact time was not helpful because of affording a lower rhodium incorporation yield (50% for $\text{Rh}^{\text{III}}\text{-M}/24(70)$) as compared to 60% for $\text{Rh}^{\text{III}}\text{-M}/6(70)$. These results are in agreement with the existence of a nonhomogeneous population of CTA^+ in as-MCM-41, most of them being released with the help of rhodium ions and, part of them, being unavailable for exchanges, may be due to stronger interactions with native silica.

Another sample, $\text{Rh}^{\text{III}}\text{-M}/6(70/70)$, was prepared according to two consecutive exchange steps using Si/Rh = 70 in each one. Such synthesis strategy corresponding to a nominal molar Si/Rh ratio of 35 was tested to increase the incorporation yield of rhodium as compared to that of $\text{Rh}^{\text{III}}\text{-M}/6(35)$. From FTIR measurements, residual surfactant molecules were still removed from the intermediate solid, $\text{Rh}^{\text{III}}\text{-M}/6(70)$, in the second step accompanied by some incorporation of rhodium. However, similar $\Delta\text{S}/\text{Rh}$

values were obtained for $\text{Rh}^0\text{-M}/6(70/70)$ and $\text{Rh}^0\text{-M}/6(35)$ (7.5 and 8, respectively) and, globally, the rhodium incorporation yield in $\text{Rh}^0\text{-M}/6(70/70)$ was only slightly higher than in $\text{Rh}^0\text{-M}/6(35)$ (35% vs 28%), which remains very low. Again, it seems that one third of CTA^+ molecules embedded in as-MCM-41 is very tightly bound to the surface.

To emphasize the importance of the surfactant molecule in rhodium insertion, two blank experiments were carried out with Rh(III) (nominal Si/Rh = 70) in ethanol at 60 °C using a surfactant-free support resulting from the pre-extraction of CTA^+ , that is, ext-MCM-41 instead of as-MCM-41. Clearly, in the absence of CTA^+ , no rhodium was incorporated after 6 h. However, addition of CTAB (0.26 g) to a mixture of ext-Si-MCM-41 (1 g) and Rh(III) in ethanol at 60 °C gave rise to a metal uptake (1.3 wt %) similar to that obtained for the $\text{Rh}^0\text{-M}/6(70)$ sample. Rhodium apparently needs CTAB help to be incorporated in resulting $\text{Rh}^{\text{III}}\text{M}(6)/y$ materials.

With three well-resolved diffraction peaks, XRD patterns of all $\text{Rh}^0\text{-M}/6(y)$ samples were consistent with the (100), (110), and (200) lattice planes of the expected hexagonal structure of MCM-41 (Fig. 2). Increasing amounts of Rh seem to lead to the decrease in the intensity of the (100) diffraction peak without modifying tremendously its half-width value meaning that the grain size of the support is maintained. However, values of the structural parameters of $\text{Rh}^0\text{-M}/6(35)$ would be slightly lower than those of calcined MCM-41 and other $\text{Rh}^0\text{-M}/6(y)$ samples as evidenced by the shift in the (100) diffraction peak of $\text{Rh}^0\text{-M}/6(35)$ toward higher values of 2 θ . The half-width of the (100) peak of $\text{Rh}^0\text{-M}(1)/120$ prepared by a direct hydrothermal treatment is a little bit larger than others.

Nitrogen adsorption–desorption isotherms (not shown here) of the different reduced solids prepared with various

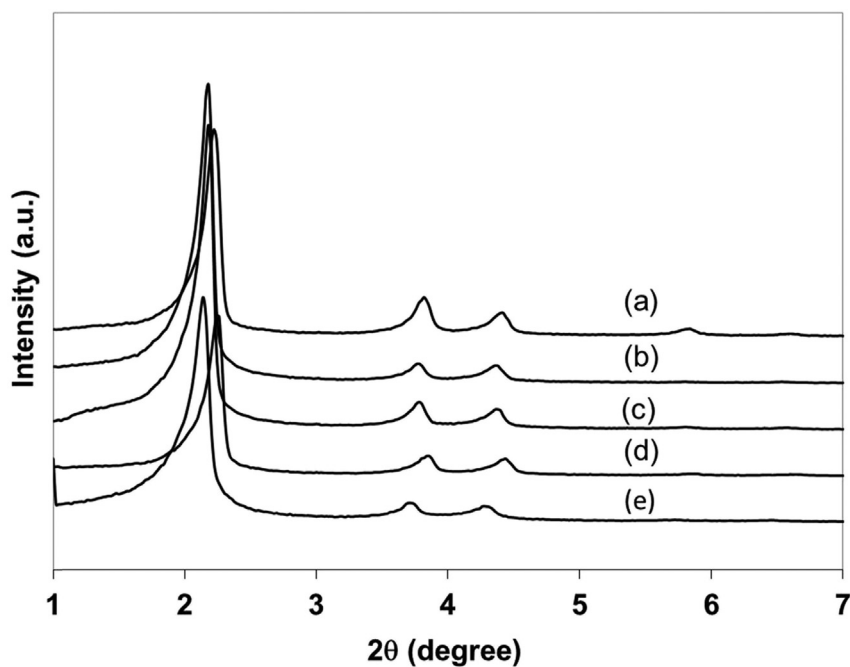


Fig. 2. XRD patterns of (a) calcined MCM-41, (b) $\text{Rh}^0\text{-M}/6(130)$, (c) $\text{Rh}^0\text{-M}/6(70)$, (d) $\text{Rh}^0\text{-M}/6(35)$, and (e) $\text{Rh}^0\text{-M}(1)/120$ samples.

Rh contents (from 0.34 to 1.4 wt % Rh) were also characteristic of materials of the MCM-41 type. Textural properties listed in Table 2 tend to show that Rh(0)-containing materials have specific surface area, pore volume, and average pore diameter values slightly inferior to those of calcined MCM-41. Textural parameters of Rh(0)-containing

materials could not help to conclude about the location of the nanoparticles due to the relatively low amount of metal loaded on the support.

TEM analysis of the most interesting sample in terms of Rh incorporation yield, that is, $\text{Rh}^0\text{-M}/6(70)$, confirmed the well-ordered pore structure with the presence of parallel

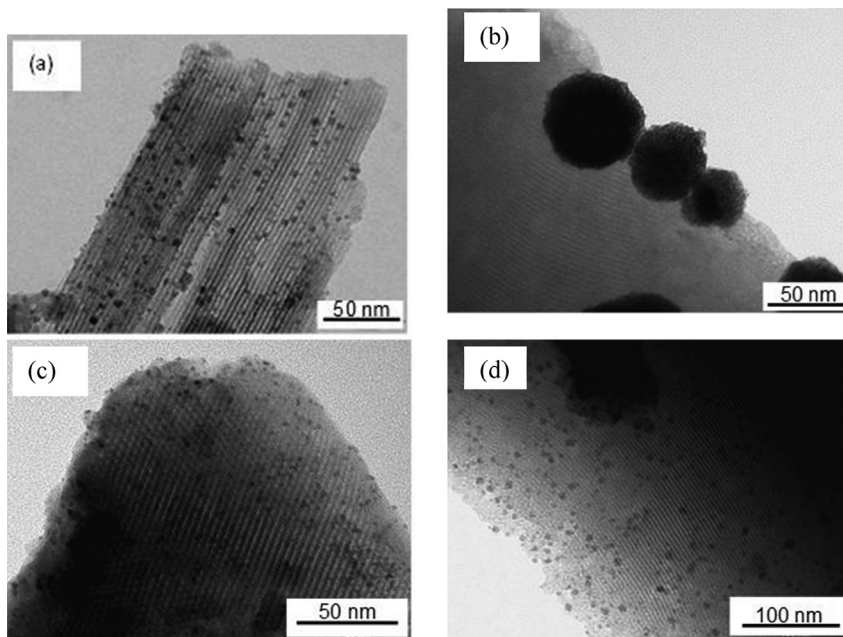


Fig. 3. TEM images of (a) $\text{Rh}^0\text{-M}/6(70)$, (b) $\text{Rh}^0\text{-M}/6(\text{Et},78,2)\text{-}$, (c) $\text{Rh}^0\text{-M}/6(\text{Et},78,2)/c$, and (d) $\text{Rh}^0\text{-M}/6(\text{Et},78,6)$ samples.

channels (longitudinal view) (Fig. 3). More importantly, most of the observed nanoparticles were characterized by a small average diameter (2–3 nm) and appeared to be spatially distributed in the direction of the channels, which is strongly consistent with their inclusion in the mesopores [41]. Nevertheless larger Rh nanoparticles (6–7 nm) could also be observed on the external surface.

3.2. Reduction by ethanol

Alcohols with high boiling points like glycols are well-known reducing agents used for the preparation of Rh(0) colloidal dispersions in ranges of temperatures between 100 and 150 °C [42]. We have checked that no Rh(0) formation was observed in EtOH in the aforementioned samples prepared at 60 °C (Rh^{III}-M/t(y) samples). In fact, reported uses of ethanol in the literature correspond to reflux temperature, 78 °C [43]. It was then tempting to look in this work at ethanol as both a solvent and a reducing agent under more appropriate conditions. Three sets of experimental conditions were tested with a nominal molar ratio Si/Rh = 70 (Table 3).

Rh³⁺ ions were either reduced

- in a second step (78 °C, 2 h) with or without isolation and calcination of the intermediate solid (Rh^{III}-M/6(70)) affording Rh⁰-M/6(Et,78,2)/c or Rh⁰-M(Et,78,2)/- samples, respectively, or
- simultaneously (78 °C, 8 h) with its introduction onto the support (Rh⁰-M'/6(Et,78,6) sample).

As expected from the study of the influence of the contact time (Table 2), longer treatments of the materials by ethanol (8 h in all instead of 6 h: Rh⁰-M/6(Et,78,2)/c and Rh⁰-M(Et,78,2)/-) lead to a decrease in the Rh uptake as compared to that of Rh⁰-M/6(70) obtained after H₂ reduction. Lower values of the textural parameters of uncalcined samples (Rh⁰-M/6(Et,78,2)/- and Rh⁰-M'/6(Et,78,6)) as compared to those of Rh⁰-M/6(Et,78,2)/c and Rh⁰-M/6(70) solids are due to the presence of residual amounts of the template not removed by a calcination step.

TEM images of Rh⁰-M(Et,78,2)/- showed a very poor dispersion of rhodium particles. About 50–100 nm metal aggregates were formed on the external surface (Fig. 3(b)), which means that Rh precursors linked to the surface are quite mobile. Such a strong reorganization was not observed after isolation and calcination of the intermediate

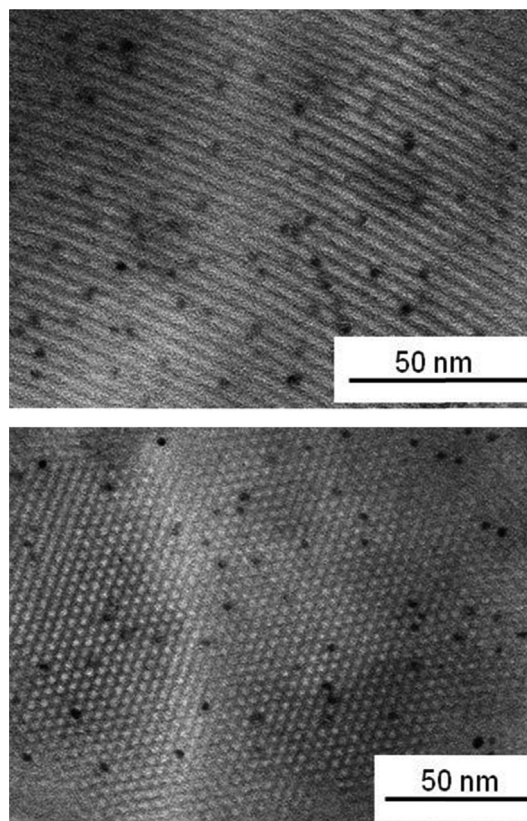


Fig. 4. TEM images (microtomy) of the Rh⁰-M(I)/120 sample.

solid before its reduction by dihydrogen (Rh⁰-M/6(70), Fig. 3(a)) or ethanol (Rh⁰-M(Et,78,2)/c, Fig. 3(c)) or when Rh insertion and reduction were carried out simultaneously (Rh⁰-M'/6(Et,78,6) (Fig. 3(d)). In these latter cases, particles are smaller but observed 6–7 nm diameter values indicate that all of them are not included in the channels of the MCM-41 support.

3.3. Comparison between direct hydrothermal synthesis and TIE Procedures

Mesoporous siliceous materials with MCM-41 pore architecture with up to 1 wt % of rhodium(0) were previously prepared in our group via a template directed hydrolysis

Table 3

Physicochemical properties of Rh⁰-M/6 samples reduced by ethanol.

Samples	Treatment			Rh (wt %)	Si/Rh exp.	S _{BET} (m ² g ⁻¹)	V _{pores} (cm ³ g ⁻¹)	D _p (nm)
	Step 1	Calcination	Step 2					
Si-MCM-41	–	–	–	–	–	800	0.70	2.6
Rh ⁰ -M/6(Et,78,2)/-	60 °C 6 h	No	78 °C 2 h	0.94	130	687	0.48	2.1
Rh ⁰ -M/6(Et,78,2)/c	60 °C 6 h	Yes	78 °C 2 h	0.72	179	861	0.75	2.7
Rh ⁰ -M'/6(Et,78,6)	78 °C 6 h	No	–	1.02	123	591	0.45	2.2

–polycondensation of TEOS in the presence of aquachlororhodium(III) complexes followed by the calcination of the template (CTAB) and the reduction of Rh(III) species by a H_2 treatment. Therefore, we were interested to determine if a better inclusion of metal nanoparticles in the mesopores could be obtained via the TIE route. Such a possibility would be based on (1) the evidence for a relationship between the incorporation of Rh and the release of CTA^+ from as-Si-MCM-41 and (2) the fact that the largest proportion of CTA^+ in as-Si-MCM-41 is located in the mesopores. Of course, such hypothesis also implies that Rh(0) and Rh(III) locations are related together (influence of the reduction treatment).

This part is focused on the comparison of $Rh^0-M/6(70)$ (this work) and $Rh^0-M(1)/120$ [6], that is, two samples containing 1.3 wt % of rhodium(0) issued from similar H_2 reduction steps (220 °C after calcination under air flow). Both materials are characterized by similar textural parameters (Table 1) and are well structured (Fig. 4). XRD patterns of $Rh^0-M/6(70)$ are almost the same as those of pure Si-MCM-41 due to the preformation of the support in the TIE method (Fig. 2). In contrast, the lattice parameter of $Rh^0-M(1)/120$ is greater than those of $Rh^0-M/6(70)$ and Si-MCM-41 as expected due to the addition of Rh^{3+} ions during the condensation of silica.

Both insertion methods of rhodium seem to have some influence on the location, dispersion, and particle size of

the resulting metal nanoparticles. Hence, microtomy TEM images of $Rh^0-M(1)/120$ showed that most of the observed nanoparticles fit with a size distribution with a mean value of 2.8 nm, which is close to the pore aperture (Fig. 4). Moreover, most of these nanoparticles were observed inside the pore channels of $Rh^0-M(1)/120$, which was not the case for $Rh^0-M/6(70)$ obtained by TIE. Thus, using MCM-41 synthesis protocols both derived from Brühwiler and Frei [39] and using exactly the same metal precursors, reduction modes and experimental metal loadings, it was clearly demonstrated that the TIE route does not lead necessarily to a better inclusion of rhodium(0). In both cases, the mean size value of included nanoparticles was similar and ultimately depends on the size of the mesopores.

3.4. Catalytic performances of the materials

$Rh(0)$ particles prepared onto mesoporous supports of the MCM-41 type were tested as catalysts in the hydrogenation of styrene at atmospheric hydrogen pressure. Three materials were considered, that is, $Rh^0-M/6(70)$, $Rh^0-M/6(Et,78,2)/c$, and $Rh^0-M/6(Et,78,2)/-$, with the aim to compare in particular the influence of the nature of the reductant on the catalytic performances. The reaction was carried out with similar substrate/Rh molar ratio (100) at room temperature in hexane. Whatever the catalyst considered, the external double bond of styrene was more

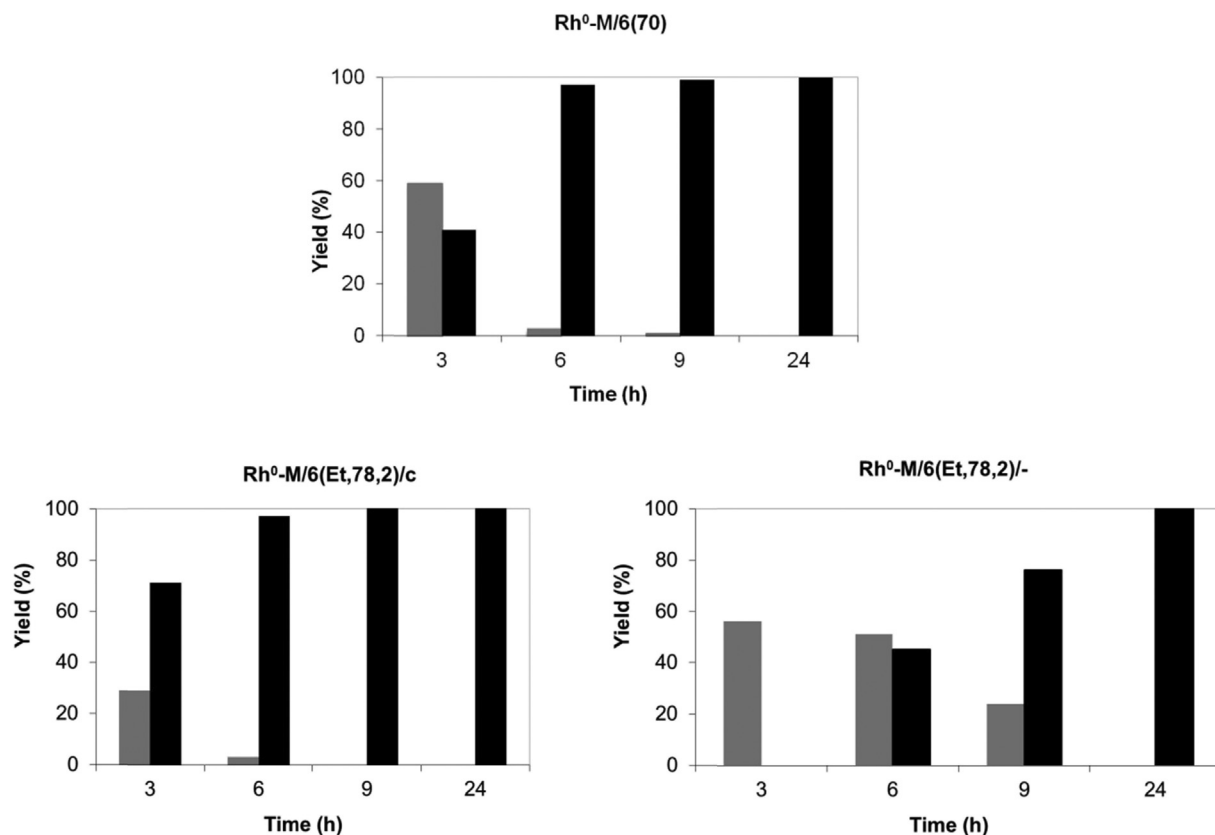
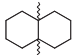
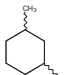
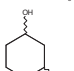
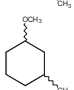


Fig. 5. Hydrogenation of styrene catalyzed by Rh^0-M samples (substrate/Rh = 100) at room temperature under atmospheric pressure of dihydrogen (EB, grey; EC, black).

Table 4
Hydrogenation of different disubstituted aromatic substrates.

Substrate	Products	Rh ⁰ -M(1)/120			Rh ⁰ -M/6(70)		
		Yield (%)	Time (h)	<i>cis/trans</i>	Yield (%)	Time (h)	<i>cis/trans</i>
Tetraline		100	1.7	89/11	100	1.0	91/09
<i>m</i> -Xylene		100	0.5	80/20	100	0.5	85/15
<i>m</i> -Cresol		100	2.5	63/37	100	1.75	60/40
3-Methylanisole		95	1.5	56/44	100	1.2	61/39

Conditions: Catalyst (100 mg), solvent (10 mL, hexane), substrate/Rh = 100, $T = 25\text{ }^{\circ}\text{C}$, $P = 1\text{ MPa}$ (H_2).

easily reduced than the aromatic ring of the molecules. Ethylcyclohexane (EC) and the intermediate, ethylbenzene (EB), were the only products detected. Histograms in Fig. 5 show the yields of EB and EC versus time for the different tested materials. Styrene was converted to EB and EC in less than 3 h in the presence of Rh⁰-M/6(70) and Rh⁰-M/6(78,2)/c samples. The reaction was completed within 24 h in all cases. Quasi-quantitative yields of EC (90–100%) were obtained in less than 6 h for Rh⁰-M/6(70) and Rh⁰-M/6(78,2)/c. Bad performances of Rh⁰-M/6(78,2)/- are linked to the presence of Rh(0) aggregates located on the external surface of the MCM-41 support.

Rh⁰-M(1)/120 and Rh⁰-M/6(70) samples were compared in the hydrogenation of four disubstituted aromatic substrates: *m*-xylene, *m*-cresol, 3-methylanisole, and tetraline (Table 4). Reactions were performed at room temperature under 1 MPa hydrogen pressure. In all of the cases considered, total hydrogenation of the aromatic ring was obtained in less than 2 h and led to the formation of *cis* and *trans* isomers (Table 4).

The *cis* compound was obtained predominantly (up to 90% in the case of decalin). For both catalysts, the *cis/trans* selectivity depends first on the structure of substrate molecules and follows the order: decalin > 1,3-dimethylcyclohexane > 3-methylcyclohexanol > 1-methoxy-3-methylcyclohexane. With the exception of *m*-cresol, *cis* selectivity is consistently higher for tests carried out with the material prepared by the TIE method. The case of *m*-cresol is particular. Indeed, it is the sole compound among those tested where significant amounts of the intermediate resulting from the addition of two moles of H_2 per mole of the substrate (3-methylcyclohexanone here) could be detected in the reaction medium [44]. Such observations suggest that the high stability of 3-methylcyclohexanone allows a “roll-over” type mechanism [45–47] to proceed affording a significant formation of the *trans* isomer of 3-methylcyclohexanol.

4. Conclusions

Impregnation of the as-MCM-41 silica by ethanolic rhodium(III) chloride solutions allowed the incorporation

of the metal with loadings of up to 1.5 wt % of the final calcined material. In ethanol, it was shown that the templating agent was still removed for longer contact times without any incorporation of additional quantities of Rh. Control experiments have shown, however, that the initial introduction of rhodium in alcohol requires the presence of the CTA⁺ cations.

The reducing action of ethanol was compared with that of dihydrogen. Clearly, whatever the reductant used, the results indicated that a strong association of Rh(III) precursors to the surface of the support through a drying and a calcination treatment of the sample before the reduction step leads to good dispersions of Rh(0). Some few nanoparticles with a size of 2–3 nm were observed, others with diameters of about 6–7 nm have also been identified for materials calcined before reduction treatments by H_2 or alcohol.

From a textural point of view, there were no significant differences between the solids obtained by direct synthesis procedures and those prepared in this study. However, structural differences allowed us to distinguish the impregnation approach (lattice parameter similar to that of the pure calcined silica) from the direct synthesis one. In this latter case, partial incorporation of Rh(III) in the walls justifies the higher value of the lattice parameter. In the hydrogenation of disubstituted aromatic compounds, the best *cis/trans* selectivities obtained with the materials resulting from impregnation also seemed to indicate that differences exist in the environment of the particles depending on whether they were introduced by an impregnation or a direct synthesis strategy.

Acknowledgments

The authors would like to thank Professor A. Roucoux and Dr. A. Denicourt for their help to carry out hydrogenation tests in their laboratory. M. Lin is also gratefully acknowledged for complementary experiments.

References

- [1] N. Zahmakran, Y. Román-Leshkov, Y. Zhang, *Langmuir* 28 (2012) 60.

- [2] V. Mevellec, A. Nowicki, A. Roucoux, C. Dujardin, P. Granger, E. Payen, K. Philippot, *New J. Chem.* 30 (2006) 1214.
- [3] C. Hubert, E. Guyonnet Bilé, A. Denicourt-Nowicki, A. Roucoux, *Green Chem.* 13 (2011) 1766.
- [4] N. Bhorali, J.N. Ganguli, *Catal. Lett.* 143 (2013) 276.
- [5] Y. Zhang, M.E. Grass, S.E. Habas, F. Tao, T. Zhang, P. Yang, G.A. Somorjai, *J. Phys. Chem. C* 111 (2007) 12243.
- [6] M. Boutros, F. Launay, A. Nowicki, T. Onfroy, V. Herledan-Semmer, A. Roucoux, A. Gédéon, *J. Mol. Catal. A: Chem.* 259 (2006) 91.
- [7] H.-B. Pan, C.M. Wai, *J. Phys. Chem. C* 114 (2010) 11364.
- [8] R. Giordano, P. Serp, P. Kalck, Y. Kihn, J. Schreiber, C. Marhic, J.-L. Duvail, *Eur. J. Inorg. Chem.* 610 (2003) 617.
- [9] S. Ganji, S.S. Enumula, R.K. Marella, K.S. Rama Rao, D. Raju Burri, *Catal. Sci. Technol.* 4 (2014) 1813.
- [10] C. Moreno-Marrodan, F. Liguori, E. Mercadé, C. Godard, C. Claver, P. Barbaro, *Catal. Sci. Technol.* 5 (2015) 3762.
- [11] M. Boutros, Z. Maoui, H. Sfihi, V. Viossat, A. Gédéon, F. Launay, *Microporous Mesoporous Mater.* 108 (2008) 247.
- [12] M. Boutros, G. Shirley, T. Onfroy, F. Launay, *Appl. Catal. A* 394 (2011) 158.
- [13] B.-I. Lee, D. Bae, J.-K. Kang, H. Kim, S.-H. Byeon, *Bull. Kor. Chem. Soc.* 30 (2009) 1701.
- [14] X. Zhang, S. Liu, H. Tong, G. Yong, *Appl. Catal. B* 127 (2012) 105.
- [15] P. Shah, A.V. Ramaswamy, K. Lazar, V. Ramaswamy, *Microporous Mesoporous Mater.* 100 (2007) 210.
- [16] S. Grosshans-Vieles, F. Tihay-Schweyer, P. Rabu, J.-L. Paillaud, P. Braunstein, B. Lebeau, C. Estournès, J.-L. Guille, J.-M. Rueff, *Microporous Mesoporous Mater.* 106 (2007) 17.
- [17] M. Yonemitsu, Y. Tanaka, M. Iwamoto, *Chem. Mater.* 9 (1997) 2679.
- [18] Y. Wang, Q. Zhang, Y. Ohishi, T. Shishido, K. Takehira, *Catal. Lett.* 72 (2001) 215.
- [19] M. Iwamoto, Y. Tanaka, J. Hirosumi, N. Kita, S. Triwahyono, *Microporous Mesoporous Mater.* 48 (2001) 271.
- [20] Q. Zhang, Y. Wang, S. Itsuki, T. Shishido, K. Takehira, *J. Mol. Catal. A: Chem.* 188 (2002) 189.
- [21] Y. Wang, Q. Zhang, T. Shishido, K. Takehira, *J. Catal.* 209 (2002) 186.
- [22] N. Lang, P. Delichere, A. Tuel, *Microporous Mesoporous Mater.* 56 (2002) 203.
- [23] Y. Wang, Y. Ohishi, T. Shishido, Q. Zhang, W. Yang, Q. Guo, H. Wan, K. Takehira, *J. Catal.* 220 (2003) 347.
- [24] Q. Zhang, W. Yang, X. Wang, Y. Wang, T. Shishido, K. Takehira, *Microporous Mesoporous Mater.* 77 (2005) 223.
- [25] T. Kawabata, Y. Ohishi, S. Itsuki, N. Fujisaki, T. Shishido, K. Takaki, Q. Zhang, Y. Wang, K. Takehira, *J. Mol. Catal. A: Chem.* 236 (2005) 99.
- [26] P. Decyck, M. Trejda, M. Ziolek, *C. R. Chimie* 8 (2005) 635.
- [27] Y. Tian, E. Ogawa, A. Ikuo, T. Shishido, Q.H. Zhang, Y. Wang, K. Takehira, S. Hasegawa, *Chem. Lett.* 35 (2006) 544.
- [28] Q. Zhang, Q. Guo, X. Wang, T. Shishido, Y. Wang, *J. Catal.* 239 (2006) 105.
- [29] A. Derylo-Marczewska, W. Gac, N. Popivnyak, G. Zukocinski, S. Pasieczna, *Catal. Today* 114 (2006) 293.
- [30] W. Gac, A. Derylo-Marczewska, S. Pasieczna-Patkowska, N. Popivnyak, G. Zukocinski, *J. Mol. Catal. A: Chem.* 268 (2007) 15.
- [31] K. Ikeda, Y. Kawamura, T. Yamamoto, M. Iwamoto, *Catal. Commun.* 9 (2008) 106.
- [32] G. Li, L. Zhong, X. Yuan, J. Wu, H. Luo, *J. Inorg. Mater.* 25 (2010) 1041.
- [33] C.M. Chanquía, A.L. Cánepa, J. Bazán-Aguirre, K. Sapag, E. Rodríguez-Castellón, P. Reyes, E.R. Herrero, S.G. Casuscelli, G.A. Eimer, *Microporous Mesoporous Mater.* 151 (2012) 2.
- [34] X.K. Li, W.J. Ji, J. Zhao, S.J. Wang, C.T. Au, *J. Catal.* 236 (2005) 181.
- [35] K. Tagaki, H. Izumida, Y. Ichihashi, S. Nishiyama, S. Tsuruya, *J. Chem. Eng. Jpn.* 38 (2005) 801.
- [36] A. Kowalczyk, A. Borchuch, M. Michalik, M. Rutkowska, B. Gil, Z. Sojka, P. Indyka, L. Chmielarz, *Microporous Mesoporous Mater.* 240 (2017) 9–21.
- [37] A. Kowalczyk, Z. Piwowarska, D. Macina, P. Kuśtrowski, A. Rokicińska, M. Michalik, L. Chmielarz, *Chem. Eng. J.* 295 (2016) 167.
- [38] T. Lehmann, T. Wolff, C. Hamel, P. Veit, B. Garke, A. Seidel-Morgenstern, *Microporous Mesoporous Mater.* 151 (2012) 113.
- [39] D. Brühwiler, H. Frei, *J. Phys. Chem. B* 107 (2003) 8547.
- [40] K. Deekamwong, J. Wittayakun, *Microporous Mesoporous Mater.* 239 (2017) 54.
- [41] J. Zhu, Z. Kónya, V. F. Puentes, I. Kiricsi, C.X. Miao, J.W. Ager, A.P. Alivisatos, G.A. Somorjai, *Langmuir* 19 (2003) 4396.
- [42] A. Roucoux, J. Schulz, H. Patin, *Chem. Rev.* 102 (2002) 3757.
- [43] Y. Wang, H. Liu, *Polym. Bull.* 25 (1991) 139.
- [44] C.V. Rode, U.D. Joshi, O. Sato, M. Shirai, *Chem. Commun.* (2003) 1960.
- [45] M. Vinięgra, N. Martin, A. Lopezgaona, G. Cordoba, *React. Kinet. Catal. Lett.* 49 (1993) 353.
- [46] R.J. Harper, C. Kamball, *J. Chem. Soc., Faraday Trans.* 90 (1994) 659.
- [47] L.M. Tang, M.Y. Huang, J.Y. Jiang, *Chin. J. Polym. Sci.* 14 (1996) 199.